Materials Transactions, Vol. 47, No. 1 (2006) pp. 59 to 62
Special Issue on Present Status of the Research on Ordered Alloys and the Application to Magnetic Devices

Order-Disorder Transformation in $L1_0$-FePd Nanoparticles Studied by Electron Diffraction

Kazuhisa Sato and Yoshihiko Hirotsu

The Institute of Scientific and Industrial Research, Osaka University, Ibaraki 567-0047, Japan

Disappearance of long-range atomic order in 10-nm-sized $L1_0$-FePd (Fe–58 at%Pd) nanoparticles has been studied by electron diffraction using a specimen heating stage attached to a transmission electron microscope. Ordered structure is kept at lowest up to 949 K, while the intensity of superlattice reflection abruptly drops at 982 K. The transformation temperature decreases by about 80 K compared to that of the bulk alloy of Fe–58 at%Pd. Nanobeam electron diffraction from a particle shows a particle size dependence of the transformation temperature and the intensity of 110 superlattice reflection largely decreases below about 15 nm in diameter at 983 K. However, a weak intensity remains in the 110 superlattice reflection even at 983 K, which is attributed to short-range order in the nanoparticles.

(Received September 2, 2005; Accepted October 19, 2005; Published January 15, 2006)

Keywords: *FePd, nanoparticle, $L1_0$, order–disorder transformation, electron diffraction, long-range order, short-range order*

1. Introduction

$L1_0$-type FePt and FePd nanoparticles have been attracting much interest due to their potential applications to ultra-high density magnetic storage media.[1,2] Hard magnetic properties of these alloy nanoparticles are originated from their tetragonal ordered structure. Actually, a correlation has been indicated between the long-range order (LRO) parameter and the magnetocrystalline anisotropy energy.[3,4] Hence the LRO parameter is a key factor when the hard magnetic properties of these $L1_0$ ordered nanoparticles are discussed. As for the small isolated alloy nanoparticles with the ordered phase, particle size dependence of the order–disorder transformation temperature has been indicated and the stabilization of the high-temperature disorder phase due to downsizing has been reported in experimental results on several alloy systems.[5–8] It was already indicated that the decrease of the Debye temperature in a small particle is responsible for such a phenomenon mentioned above.[6] However, few experimental studies concerning the direct observation of the order–disorder transformation in alloy nanoparticles exists until now.[9] Actually, order–disorder transformation usually takes place at a few hundred degree of centigrade and such a high temperature condition will cause not only the transformation but also coalescence of nanoparticles. As for the binary FePd alloy, for example, the transformation temperature indicated in the phase diagram[10] is around 1063 K for Fe–58 at%Pd alloy. Therefore the preparation of well-isolated alloy nanoparticles with less coalescence growth during the heat treatment is necessary for the investigation of the order–disorder transformation as a function of particle size precisely. Present authors have developed a fabrication method of well-isolated FePd nanoparticles with less coalescence growth.[11] In our previous study, it was confirmed that the mean particle size and the size distribution observed in the as-deposited condition was conserved even after annealing at 873 K for 36 ks.

In this study, we have investigated the order–disorder transformation of 10-nm-sized FePd nanoparticles by electron diffraction using an *in-situ* annealing technique.

2. Experimental Procedure

FePd nanoparticles were fabricated by successive deposition of Pd and Fe onto NaCl(001) substrates kept at 673 K using an electron-beam evaporation apparatus. In the specimen fabrication process, Pd nanoparticles act as nucleation sites for successively deposited Fe nanoparticles and formed Fe/Pd nanocomplex particles in the as-deposited condition. Because of the epitaxial growth of Pd onto NaCl, and Fe onto Pd, the following orientation relationships[11] exist: $\langle 011\rangle_{Pd} \| \langle 011\rangle_{NaCl}$, $\{100\}_{Pd} \| \{100\}_{NaCl}$, and $\langle 100\rangle_{Fe} \| \langle 100\rangle_{Pd}$, $\{011\}_{Fe} \| \{010\}_{Pd}$. After the deposition of Fe, we further deposited an amorphous Al_2O_3 thin film to protect the particles from oxidation and also to isolate the particles to each other. Post-deposition annealing at 873 K for 3.6 ks was performed in order to promote the alloying and the atomic ordering reaction of Fe and Pd. According to our previous study,[12] post-deposition annealing at 873 K for 3.6 ks lead to the formation of single $L1_0$ phase with the LRO parameter of 0.65 for 10-nm-sized Fe–58 at%Pd nanoparticles. Details of fabrication procedure are shown in our previous article.[11] Structure and morphology of the FePd nanoparticles were characterized by *in-situ* transmission electron microscope (TEM) observation, selected area electron diffraction (SAED) and nanobeam electron diffraction (NBD) using a TEM operated at 300 kV (JEOL, JEM-3000F). Imaging plates (Fuji Film, FDL-UR-V) were used as a recording media. In this study, particle size was defined as arithmetical mean of the major and the minor axes of ellipse, and the particle size distribution is represented by a log-normal type distribution function. The total number of particles measured was more than 250 for each TEM image. During the *in-situ* heating of the specimen film in the TEM, electron beam was shut out by closing the gate-valve, and also applied current to the objective pole-piece was switched off in order to remove the magnetic field applied perpendicular to the film plane. A Pt–Pt13%Rh thermocouple attached to the specimen heating stage was used for temperature measurements. For the purpose of calibrating the thermocouple, atomic ordering temperatures of the as-deposited Fe/Pd and Fe/Pt nanocomplex particles observed by *in-situ* annealing were

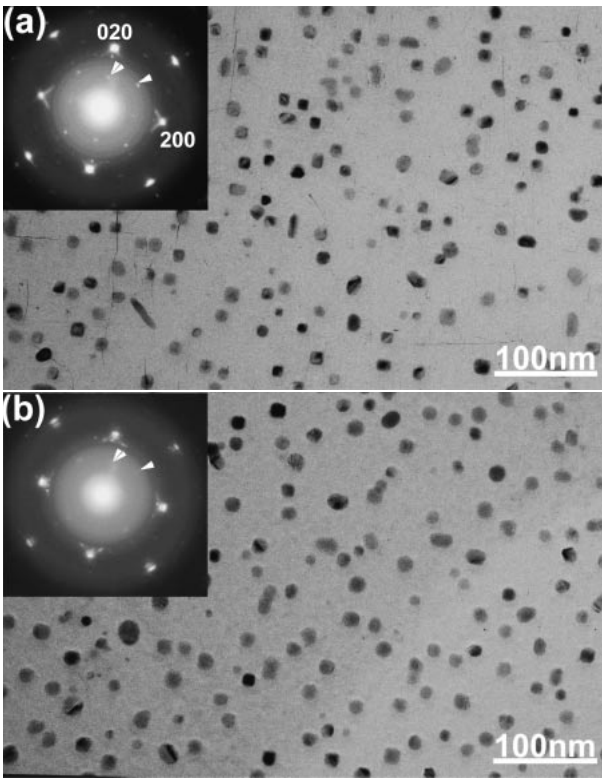

Fig. 1 BF-TEM images and the corresponding SAED patterns for FePd nanoparticles observed at (a) 295 K and (b) 982 K, respectively. An arrow head and double arrows in Fig. 1(a) indicate the 110 and 001 superlattice reflections, respectively. These superlattice reflections of the $L1_0$ type ordered structure almost disappeared at 982 K [Fig. 1(b)].

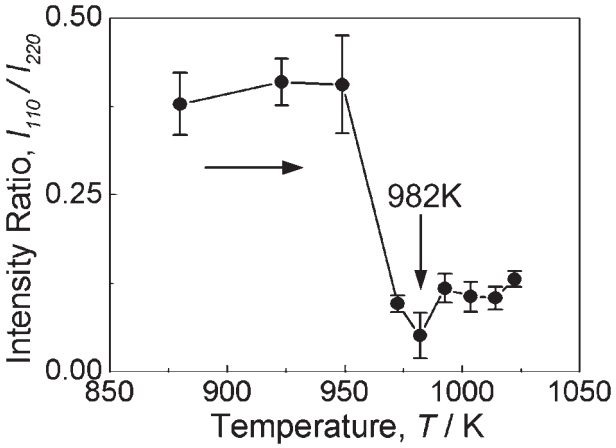

Fig. 2 Annealing temperature dependence of the intensity ratio I_{110}/I_{220} obtained by the intensity analyses of the SAED patterns. The slight increase of the intensity ratio at the temperatures between 880 and 923 K is due to the evolution of the LRO. At 982 K, the intensity ratio abruptly decreases while a weak intensity still remains.

compared to those obtained by ex-situ annealing using an electric furnace, however, there observed no apparent differences between them. Compositional analysis was performed by an energy dispersive X-ray spectrometer attached to the TEM. The specimens used in the present experiment had the average composition of 58 at%Pd.

3. Results and Discussion

Figure 1 shows bright-field (BF) TEM images and the corresponding SAED patterns of the FePd nanoparticles observed at 295 and 982 K, respectively. The mean particle size of this specimen at 295 K was 12.0 nm with deviation $\ln\sigma$ of 0.13. An arrow head and double arrows in Fig. 1(a) indicate the 110 and 001 superlattice reflections, respectively. Note that the superlattice reflections observed at 295 K disappeared at 982 K without changing their particle size and particle density significantly. Actually, the intensity ratio of 110 superlattice reflection to 220 fundamental reflection (hereafter, I_{110}/I_{220}) abruptly drops at a temperature between 949 and 982 K as shown in Fig. 2, indicating the disordering due to the order–disorder transformation. The averaged heating rate at the temperatures between 880 and 1022 K shown in Fig. 2 was about 0.037 K/s, and the SAED observation was performed within about 300 s at each temperature. The intensities of 110 and 220 reflections were measured from the intensity profile, which was measured along [110]* direction on the SAED pattern observed at each temperature. The beam incidence was parallel to [001] for the FePd nanoparticles with their crystallographic c-axes oriented normal to the film plane. When the intensity ratio abruptly decreased at 982 K, the mean particle size was 13.5 nm ($\ln\sigma = 0.16$) in diameter. That is, the transformation temperature of the FePd nanoparticles decreased by 80 K compared to that of the bulk alloy of 58 at%Pd according to the binary phase diagram.[10] It should be noted that the intensity ratio decreased at the temperatures between 949 and 982 K with a slight gradient, while the bulk CuAu I alloy,[13] which undergoes the FCC-$L1_0$ phase transformation like FePd, shows a rapid drop of the LRO parameter from almost unity to zero at the transformation temperature. On the contrary, continuous decrease of the order parameter in a wide temperature range has been reported in 3-nm-sized FePt[14] and 2–3-nm-sized Cu_3Au nanoparticles[15] by Monte Carlo simulations considering the interatomic interactions up to the third nearest neighbors, and the second nearest neighbors, respectively. Note that the order–disorder transformation of the present FePd nanoparticles with mean size of 13.5 nm is found to be similar to that of the bulk alloy rather than those of 2 or 3-nm-sized nanoparticles[14,15] from the viewpoint of the considerably abrupt change of the intensity ratio. The observed slight gradient of the intensity ratio at the transformation temperature can be attributed to the distribution of the transformation temperature due to the particle size distribution. Remarkable feature appeared in Fig. 2 is the residual weak intensity ratio at 982 K, and it gradually increased with temperature up to 1022 K. Particle size gradually increased on heating and it reached to 14.6 nm ($\ln\sigma = 0.18$) in mean diameter at 1022 K, which is about 8% larger than that observed at 982 K (13.5 nm). The observed gradual increase of the intensity ratio above 982 K is attributed to the evolution of the LRO due to a slight particle growth by coalescence as mentioned above, since the transformation temperature is considered to depend on the particle size. Actually, FePd nanoparticles with sizes larger than 15 nm in diameter showed clear superlattice reflections in NBD patterns even at 983 K, which will be shown later.

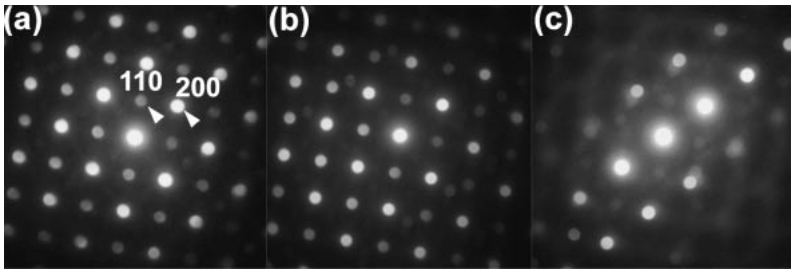

Fig. 3 NBD patterns for FePd nanoparticles observed at (a) 923 K, (b) 948 K and (c) 983 K, respectively with beam incidence of [001]. The particle sizes observed in (a), (b) and (c) are all 12 nm in diameter. Disappearance of the 110 superlattice reflection is clearly seen in Fig. 3(c).

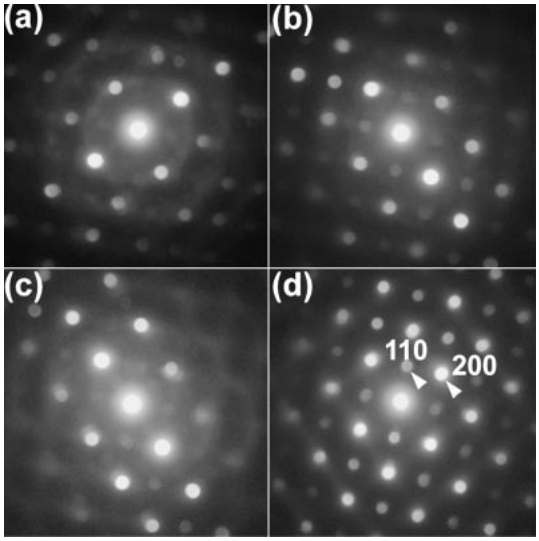

Fig. 4 NBD patterns for FePd nanoparticles observed at 983 K with beam incidence of [001]. The observed particle sizes are (a) 11.5 nm, (b) 13 nm, (c) 14 nm, and (d) 15 nm, respectively. Superlattice reflections of 110 are almost invisible or very weak for FePd nanoparticles with sizes below 14 nm, while clear intensity is visible in a 15 nm-sized particle.

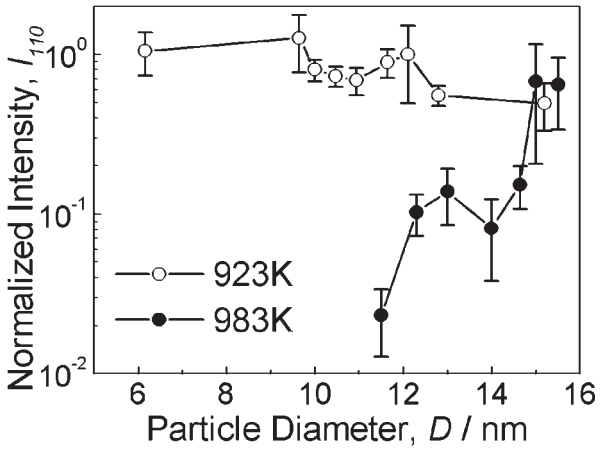

Fig. 5 Particle diameter dependence of the normalized 110 intensity measured at 923 K (open circle) and 983 K (solid circle), respectively. The large decrease of the superlattice reflection intensity is visible at 983 K, while weak intensities still remains due to SRO.

Note that the population of the particles with their sizes larger than 15 nm was 29% at 982 K, while it increased to 46% at 1022 K in the specimen used for *in-situ* SAED observation. It is obvious that such an increase of the intensity ratio above the transformation temperature, that is, evolution of the LRO, must vanish when the specimen particles are free from coalescence growth during the heating. The remained intensity ratio at 982 K can be explained by the existence of the particle size distribution as mentioned above.

Besides the particle size distribution there is a possibility for explaining the remained intensity ratio by the residual short-range order (SRO) above the transformation temperature,[13] which should be clarified by the NBD intensity analyses. NBD patterns were observed at the temperatures between 923 and 983 K. The mean heating rate was about 0.13 K/s, and the NBD observation was performed within 7.2 ks at each temperature. Mean particle size of the observed specimen was 11.3 nm ($\ln\sigma = 0.23$) at 923 K and it slightly increased to 11.5 nm ($\ln\sigma = 0.21$) at 948 K and 11.9 nm ($\ln\sigma = 0.21$) at 983 K, respectively. Particle size change of this specimen during the heating is smaller than that of the specimen used in the SAED observation. Figure 3 shows the three NBD patterns observed at 923 K (3a), 948 K (3b) and 983 K (3c), respectively from three different FePd nanoparticles but with the same particle size of 12 nm in diameter. Superlattice reflections are clearly seen in the NBD patterns obtained at 923 and 983 K. By contrast, superlattice reflections almost disappeared at 983 K, which agrees well to the result by SAED analyses shown in Fig. 2. Then we examined the particle size dependence of the order–disorder transformation temperature. Figure 4 shows the four kinds of NBD patterns observed at 983 K from particles with diameters of (a) 11.5 nm, (b) 13 nm, (c) 14 nm and (d) 15 nm, respectively. At this temperature the intensity of superlattice reflection largely decreased as shown in Fig. 2. Actually, the intensities of superlattice reflections are very weak or almost invisible for the particles with sizes below 14 nm [Figs. 4(a), (b) and (c)]. However, superlattice reflections are still clearly seen in the NBD pattern taken from the FePd nanoparticle with a size of 15 nm. It should be noted that NBD patterns in Fig. 4 indicates a particle size dependence of the order–disorder transformation temperature in the FePd nanoparticles. Figure 5 shows the particle size dependence of the 110 superlattice reflection intensity measured at 923 K (open circle) and 983 K (solid circle), respectively. The intensities were normalized by the 110 intensity of a 12-nm-sized FePd nanoparticle observed at 923 K with a sufficient LRO. It is clearly shown that particle

size dependence of I_{110} is small at 923 K, although multiple scattering of electrons as well as the thickness change due to the particle size difference will arise a particle size dependence of I_{110}[12,16] to some extent. By contrast, I_{110} largely decreases at 983 K as the particle size is reduced below about 15 nm in diameter. However, very weak intensity still remains at 983 K for the particles smaller than 15 nm, indicating the existence of SRO in these FePd nanoparticles. In case that SRO exists in a disordered alloy, the intensity due to SRO (I_{SRO}) is proportional to the following Fourier transform ($\alpha(h_1h_2h_3)$) of the Warren–Cowley parameter, $\alpha(lmn)$:[17]

$$\alpha(h_1h_2h_3) = \sum_l \sum_m \sum_n \alpha(lmn) \cos \pi l h_1 \times \cos \pi m h_2 \cos \pi n h_3, \quad (1)$$

where h_1, h_2, h_3 are continuous variables, l, m, n are integers, $\alpha(lmn)$ the order parameter for neighbors at a distance $r_n = la_1/2 + ma_2/2 + na_3/2$ with the usual principal axes a_1, a_2, a_3. Magnitude of the parameter $|\alpha(lmn)|$ takes unity for the perfect $L1_0$ ordering and it decreases towards zero as the SRO vanishes. Then we calculated the intensity ratio of SRO to LRO ($I_{\mathrm{SRO}}/I_{\mathrm{LRO}}$) for the 110 reciprocal point using $\alpha(lmn)$ values up to 8th nearest neighbors reported by Roberts for CuAu I structure.[13] Here, I_{LRO} corresponds to I_{SRO} for the perfect order. As a result, $I_{\mathrm{SRO}}/I_{\mathrm{LRO}} \approx 0.04$–$0.14$ was obtained, which agrees well to the normalized I_{110} values obtained at 983 K in the present experiment as shown in Fig. 5. It is concluded that the observed weak 110 intensity in NBD at 983 K arises from SRO in the FePd nanoparticles.

Note that particles larger than about 15 nm in diameter showed the strong 110 intensity comparable to those of 923 K. Hence, the FePd nanoparticles with sizes less than 15 nm, which corresponds to 78% of the particles in this specimen, showed a lower transformation temperature than that of the bulk alloy. It is clearly shown that there is a particle size dependence of the order–disorder transformation temperature of 10-nm-sized FePd isolated nanoparticles. The remained superlattice reflection intensity in the NBD patterns is attributed to the existence of SRO, while that of the SAED patterns include both the effects of the particle size distribution and SRO.

4. Conclusion

The order–disorder transformation of 10-nm-sized FePd nanoparticles has been studied by electron diffraction using a specimen heating stage attached to TEM. It is found that the order–disorder transformation temperature for isolated FePd nanoparticles with mean particle size of 13.5 nm is reduced by about 80 K than that of the bulk alloy. The order–disorder transformation of the present FePd nanoparticles is similar to that of the bulk alloy from the viewpoint of the abrupt change of the intensity ratio. Particle size dependence of the transformation temperature is studied by NBD and found that the intensity of 110 superlattice reflection largely decreases when the particle size smaller than about 15 nm at 983 K, however, a weak 110 intensity remains even above the transformation temperature due to the existence of SRO. From the technological viewpoint, it is also suggested that an annealing for atomic ordering should be done at a temperature lower than 949 K for 10-nm-sized FePd nanoparticles.

Acknowledgment

This study was partly supported by the Grant-in-Aid for Scientific Research (S) (Grant No. 16106008) and the Grant-in-Aid for Young Scientists (B) (Grant No. 17760531) from the Ministry of Education, Culture, Sports, Science and Technology, Japan.

REFERENCES

1) D. Weller and M. F. Doerner: Annu. Rev. Mater. Sci. **30** (2000) 611–644.
2) For example, *Abstract of the Conference on L1$_0$ Ordered Intermetallic and Related Phases for Permanent Magnet and Recording Applications, Copper Mountain, Colorado, August 15–20, 2004* (Engineering Conference International, Brooklyn, NY, 2004).
3) H. Kanazawa, G. Lauhoff and T. Suzuki: J. Appl. Phys. **87** (2000) 6143–6145.
4) S. Okamoto, N. Kikuchi, O. Kitakami, T. Miyazaki, Y. Shimada and K. Fukamichi: Phys. Rev. B **66** (2002) 024413_1–024413_9.
5) T. Kizuka, N. Mitarai and N. Tanaka: J. Mater. Sci. **29** (1994) 5599–5606.
6) H. Yasuda and H. Mori: Z. Phys. D; At., Mol. Clusters **37** (1996) 181–184.
7) H. Pan, S. Fukami, J. Yamasaki and N. Tanaka: Mater. Trans. **44** (2003) 2048–2054.
8) Y. K. Takahashi, T. Ohkubo, M. Ohnuma and K. Hono: J. Appl. Phys. **93** (2003) 7166–7168.
9) T. Tadaki, A. Koreeda, Y. Nakata and T. Kinoshita: Surf. Rev. Lett. **3** (1996) 65–69.
10) T. B. Massalski, H. Okamoto, P. R. Subramanian and L. Kacprzak (ed.): *Binary Alloy Phase Diagrams*, 2nd ed., (ASM International, Materials Park, Ohio, 1990), p.1751.
11) K. Sato and Y. Hirotsu: J. Appl. Phys. **93** (2003) 6291–6298.
12) K. Sato, Y. Hirotsu, H. Mori, Z. Wang and T. Hirayama: J. Appl. Phys. **97** (2005) 084301_1–084301_7.
13) B. W. Roberts: Acta Met. **2** (1954) 597–603.
14) R. V. Chepulskii, J. Velev and W. H. Butler: J. Appl. Phys. **97** (2005) 10J311_1–10J311_3.
15) T. Tadaki, T. Kinoshita, Y. Nakata, T. Ohkubo and Y. Hirotsu: Z. Phys. D; At., Mol. Clusters **40** (1997) 493–495.
16) K. Sato, Y. Hirotsu, H. Mori, Z. Wang and T. Hirayama: J. Appl. Phys. **98** (2005) 024308_1–024308_8.
17) J. M. Cowley: J. Appl. Phys. **21** (1950) 24–30.